Front. Earth Sci. 2023, 17(1): 135−144
https://doi.org/10.1007/s11707-022-0991-4

RESEARCH ARTICLE

Experimental study on the coupling effect of pore-fracture system and permeability controlled by stress in high-rank coal

Jiang HAN[1,2], Caifang WU (✉)[1,2], Lu CHENG[3]

1 Key Laboratory of Coalbed Methane Resources and Reservoir Formation (Ministry of Education of China), China University of Mining and Technology, Xuzhou 221116, China
2 School of Resources and Geoscience, China University of Mining and Technology, Xuzhou 221116, China
3 China United Coalbed Methane Corporation, Ltd., Beijing 100016, China

Abstract During the coalbed methane (CBM) exploitation, the reservoir permeability can be affected by the effective stress that varies with the reservoir fluid pressure, which is a complex, dynamic and significant engineering problem. To analyze the response characteristics of the pore-fracture system by the changing stress, this work simulated reservoir and fluid pressures during the exploitation by adjusting confining pressure and displacement pressure. Stress sensitivity experiments under different effective stresses were conducted to systematically study the stage variation characteristics of porosity and permeability of coal. The results show that the permeability decreases exponentially with the increase in effective stress, consistent with previous studies. However, the porosity shows a V-shaped trend, which is different from the traditional understanding that it would decrease continuously with rising effective stress. These variation characteristics (of porosity and permeability above) therefore result in a phased porosity sensitivity of coal permeability (P_{PS}). Moreover, the stress sensitivity of the samples was evaluated using the permeability damage rate method (M_{PDR}) and the stress sensitivity coefficient method (M_{CSS}), both of which showed that it ranges from the degree of strong to extremely strong. When the effective stress is lower than 5–6 MPa, the stress sensitivity of the coal reservoir drops rapidly with effective stress rising; when it is higher than 5–6 MPa, the change in stress sensitivity tends to flatten out, and the stress sensitivity coefficient (C_{SS}) goes down slowly with rising effective stress. Finally, suggestions are proposed for the drainage scheme of CBM wells based on the experimental results.

Received January 5, 2021; accepted March 31, 2022

E-mail: caifangwu@sina.com

Keywords stress sensitivity, porosity sensitivity, permeability, high-rank coal, effective stress

1 Introduction

Unconventional natural gas development has become a major issue to be addressed at a time of international energy scarcity and rising carbon emissions (Xie et al., 2017; Tao et al., 2019a, 2019b). Coal, a porous medium, is suitable for coalbed methane (CBM) development, but its low porosity and permeability make it difficult to transport reservoir fluid, profoundly restricting the production of CBM (Tao et al., 2018; Chen et al., 2021b, 2021c; Ye et al., 2022).

Previous studies have considered that the porosity and permeability of coal mainly were determined by the geometric distribution of pore-fracture systems (Liu et al., 2011b; Wang et al., 2011), and affected by reservoir temperature, water saturation, reservoir fluid type, and effective stress in the reservoir at the same time (Jasinge et al., 2011; Wang et al., 2011; Guo et al., 2014; Wang et al., 2014b; Li et al., 2014; Zhang et al., 2016b; Guo et al., 2017; Liu et al., 2017), while they also showed a non-linear variation with stress (Chen et al., 2011, 2012; Meng and Li, 2013; Zhang et al., 2015; Chen et al., 2021a). Zhang et al. (2019b) found a positive correlation between the permeability and porosity of coal, and concluded that it was caused by the change of the effective flow path since they both went down when the effective flow path was contracted. They also found that coal with high initial porosity had more significant porosity and permeability changes under stress.

The dynamic permeability during CBM extraction is a complex coupled problem that is mainly influenced by

effective stress, matrix shrinkage effect, and the Klinkenberg effect, among which, the effective stress is considered to be the main influencing factor and the only negative one (Liu et al., 2011a; Wang et al., 2014a, 2014b; Yao et al., 2014; Chen et al., 2015; Zhang et al., 2015, 2017b; Ju et al., 2017; Niu et al., 2018). Numerous mathematical models were developed to predict the dynamic permeability change during the CBM well production (Liu and Rutqvist, 2010; Pan et al., 2010; Mitra et al., 2012; Aziz et al., 2013; Özgül et al., 2017), but unfortunately, it's impossible to widely apply them to CBM well production because of their limitations.

In the process of CBM exploitation, the stress sensitivity of the coal reservoir changes as the fluid transports (Xiao et al., 2021). The stress sensitivity has been studied extensively by previous researchers who concluded that coal was a porous medium with high-stress sensitivity. As stress sensitivity is influenced by several factors: reservoir fluid, water saturation, reservoir components, reservoir temperature, and pore-fracture space distribution characteristics (Somerton et al., 1975; Durucan and Edwards, 1986; Meng et al., 2015; Xiao et al., 2016; Geng et al., 2017), many methods have been proposed to characterize it, which can be categorized into two types, i.e., stress sensitivity coefficient method (M_{CSS}) and permeability damage rate method (M_{PDR}) (Somerton et al., 1975; Jones and Owens, 1980; Durucan and Edwards, 1986; McKee et al., 1988; Xiao et al., 2016). Some researchers investigated the variation of stress sensitivity with effective stress in coal reservoirs under different in situ stresses and found that, under low in situ stress, coal seams had higher stress sensitivity with ascending effective stress; while the sensitivity became lower under high in situ stress (Meng and Li, 2013; Meng et al., 2015).

The porosity sensitivity of permeability (P_{PS}) refers to the characteristic of coal permeability changing with porosity, which relates stress sensitivity with the characteristics of pore-fracture space change and is important for the investigation of the stress sensitivity of pore-fracture space in coal reservoirs (Zhang et al., 2019b). Therefore, deepened understanding of the P_{PS} of coal can provide theoretical support for permeability enhancement projects such as pore size and pore connectivity adjustment. In contrast to stress sensitivity, which has been extensively studied, the P_{PS} of coal has gained little attention (Zhang et al., 2015). The P_{PS} of coal, commonly defined as a constant of 3 or a multiple of 3 (Cui and Bustin, 2005; Wang et al., 2013; Shi et al., 2014), is actually a variable controlled by the distribution characteristics and compressibility of the pore-fracture system and effective stress, which reveals the limitations of much previous research.

The stress sensitivity and P_{PS} of coal significantly affect the fluid seepage within coal reservoirs, determining CBM production capacity. Under different effective stresses, both coal matrix and pore-fracture space are nonlinearly compressed (Zhao et al., 2016; Wang et al., 2018a, 2018b; Ai et al., 2021). Therefore, it is meaningful to comprehensively understand the stress sensitivity and P_{PS} of coal reservoirs. Previous studies on reservoir permeability during CBM well exploitation have mostly focused on the stress sensitivity evaluation with a single value, but few have focused on the stage variation characteristics of reservoir stress sensitivity.

In this work, stress sensitivity experiments were carried out to study the correlations between confining pressure, pore pressure, porosity, and permeability, analyze the P_{PS} of coal and the variation of porosity and permeability with different effective stresses, and investigate the stage variation of stress sensitivity during CBM well drainage based on the real discharge conditions of CBM wells. Finally, suggestions were given for the CBM well drainage scheme.

2 Experiments and methodology

2.1 Sample preparation

No. 3 coal of the Shanxi Formation in the southern Qinshui Basin, China, is structurally simple and thick. It is not only the main mining target of coalfields, but also the main gas-producing layer of CBM wells in this area (Meng et al., 2018; Wang et al., 2020). Fresh No. 3 coal samples were collected from the Sihe coalfield in this area in a cylindrical shape with a dimension of 25 mm in diameter × 50 mm in length by drilling in parallel to the seam on a lump of large intact coal (Fig. 1).

These cylindrical samples were used for porosity and permeability testing under different confining and displacement pressures. The basic parameters of the samples were measured using coal core residue from drilling (Table 1). The results show that the samples are typical high-rank coal.

2.2 Testing equipment and experimental procedure

Porosity and permeability were tested using the SCMS-E

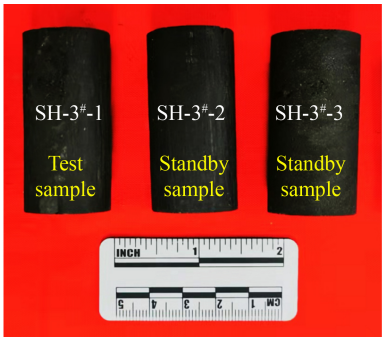

Fig. 1 Cylindrical samples for experiments.

Table 1 Basic information of samples for experiments

Sample	Macrolithotype and texture	Burial depth/m	Industrial analysis				$R_{o,max}$/%
			M_{ad}/%	A_d/%	V_{daf}/%	$S_{t,d}$/%	
SH-3#	Black semi-bright coal banded or homogeneous	<1200	2.60	13.76	6.69	0.32	3.86

Notes: M_{ad} is moisture content at air-dried basis; A_d is ash yield at dried basis; V_{daf} is volatile content at dried and ash-free basis; $S_{t,d}$ is total sulfur content at dried basis; $R_{o,max}$ is maximum reflectance of vitrinite.

automatic core multi-parameter measurement system, and the schematic diagram is shown in Fig. 2. This equipment can be used to measure gas porosity from 0.1% to 30% and gas permeability from 10^{-5} to 2000 (10^{-3} μm^2). Helium, a gas with physical properties close to those of CH_4 and considered by other researchers as a substitute for CH_4 in porosity and permeability tests, was chosen as required by the laboratory safety regime (Pan et al., 2010; Geng et al., 2017; Shaw et al., 2019).

The overburden pressure on the target reservoir varies with the burial depth in different CBM wells, and the reservoir fluid pressure changes continuously and mostly decreases during the CBM well exploitation. The confining pressure was set by simulating the real reservoir conditions at the location for sample collection, where the average pressure gradient was 7.1 MPa/km, and the burial depth was shallower than 1200 m (Meng et al., 2015). The displacement pressure was designed based on the bottom flow pressure in CBM wells. The values of confining pressure were 3.0, 4.0, 6.0, 8.0, and 10.0 MPa and the values of displacement pressure were 2.0, 3.0, 5.0, and 7.0 MPa. 19 sets of experiments were set up as shown in Fig. 3. To exclude the influence of temperature on the experimental results, the constant temperature cabinet was set at 25°C. Each stress point was kept in equilibrium at least 60 min before testing to ensure the accuracy of the measurement results. Additionally, the pore pressure was approximately equal to half of the displacement pressure, as the tiny outlet pressure was neglectable.

2.3 Methodology

All processes involving fluid transport in coal reservoirs are influenced by porosity and permeability (Zhang et al., 2015, 2016a, 2017b). Investigating the relationship between porosity and permeability will help to understand the details of fluid flow from macroscopics.

The correlation equation (Eq. (1)) between porosity and permeability was proposed by previous researchers based on the matchstick model and fracture flow cubic law (Zhang et al., 2019b):

$$\frac{k}{k_0} = \left(\frac{\phi_e}{\phi_{e_0}}\right)^3, \tag{1}$$

where k is the permeability of coal under stress, 10^{-3} μm^2; k_0 is the initial permeability of coal, 10^{-3} μm^2; ϕ_e is the porosity of coal under stress, dimensionless; ϕ_{e_0} is initial porosity of coal, dimensionless.

Some experts have doubted the cubic relationship (Gu and Chalaturnyk, 2010; Zhang et al., 2015). To accurately evaluate the correlation between permeability and porosity, a new parameter was introduced based on Eq. (1), and thus Eq. (2) was obtained (Zhang et al., 2019b):

$$\frac{k}{k_0} = \left(\frac{\phi_e}{\phi_{e_0}}\right)^{\alpha_H}, \tag{2}$$

where, α_H is used to characterize the P_{PS} of coal, dimensionless, calculated in Eq. (3). Other parameters are explained in the list of symbols as well as the following equation:

$$\alpha_H = \frac{\lg(k/k_0)}{\lg(\phi/\phi_0)}. \tag{3}$$

There are two methods commonly used to evaluate stress sensitivity, summarized as M_{PDR} and M_{CSS}, respectively (Xiao et al., 2016; Zhang et al., 2019a). Eq. (4)

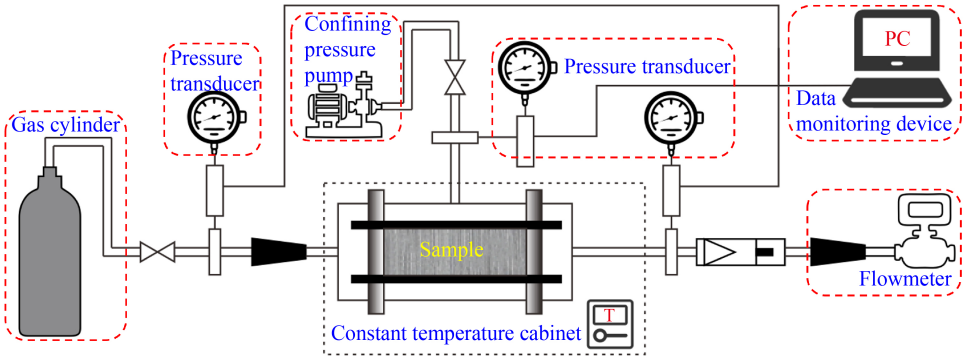

Fig. 2 Schematic diagram of the test equipment for porosity-permeability co-metering.

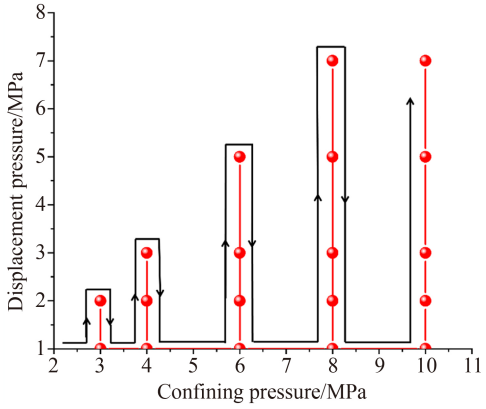

Fig. 3 Schematic diagram of the experiment.

below is suitable for M_{CSS}, and the evaluation criteria are shown in Table 2 (Zhang et al., 2019a; Shao et al., 2020; Han et al., 2022), while Eq. (5) is suitable for the calculation of M_{PDR}, and the evaluation criteria are listed in Table 3 (Meng et al., 2015):

$$S_s = \frac{1-(k/k_0)^{1/3}}{\lg(\sigma_e/\sigma_{e0})}, \tag{4}$$

$$D_k = \frac{k_0 - k}{k_0} \times 100\%, \tag{5}$$

where S_s is stress sensitivity coefficient, dimensionless; σ_e is effective stress, MPa; σ_{e0} is initial effective stress, MPa; D_k is permeability damage rate, dimensionless.

3 Experimental results and discussion

3.1 Porosity and permeability of coal under different stresses

The experiments conducted are shown in Fig. 3 and the results are shown in Fig. 4. The porosity and permeability characteristics under different confining pressures and pore pressures were compared. Meanwhile, quantitative analysis was conducted on the various characteristics of pore-fracture space under different overburden pressures during fluid pressure change. Terzaghi's effective stress law, which considers the effective stress coefficient as 1, was used to analyze the relationship between the effective stress on porosity and permeability.

As shown in Fig. 4(a), the porosity of coal shows a first decreasing and then increasing trend with the increase of pore pressure, and the "turning point" mostly occurs when pore pressure ranges from 1 to 1.5 MPa. The porosity of coal at the final stage is lower than that at the initial stage (except that at the confining pressure of 3 MPa) The reason for this is that the experimental displacement pressure must be lower than the confining pressure, so only two stress points were tested at the confining pressure of 3 MPa, and both stress points were before the "turning point". At an equal pore pressure, when confining pressure increases, porosity will significantly decrease, which is particularly obvious after the "turning point".

Previous studies have concluded that the porosity of coal would increase with pore pressure at a constant confining pressure because the fluid with high pressure bore part of stress instead of the coal matrix, and the partially compressed and closed pore-fracture space would be re-opened, but no attention was paid to the specific stage where porosity would decrease (before the "turning point"). We believe that the non-homogeneity of coal and the complex pore distribution characteristics play major roles in this regard. With low displacement pressure, the test gas cannot fully occupy all the pore-fracture space in the coal, thus leading to the partial closure of the pore-fracture space with ascending confining pressure. When the displacement pressure exceeds the "critical point", the gas can occupy more pore-fracture space, at which time, the seepage paths closed by confining pressure will be re-opened gradually. This complex process is the reason why porosity fluctuates. When an advantageous seepage path is formed, it is difficult for the test gas to open more pore-fracture space, and the porosity will stop increasing. Still, some previously closed pore-fractures will remain unchanged at this time, which explains why the effective porosity at the final stage is lower than that at the initial stage.

In Fig. 4(b), the permeability increases with pore pressure under a constant confining pressure, but its increment gradually goes down with the increase of

Table 2 Evaluation criteria of stress sensitivity by stress sensitivity coefficient method

Sensitivity coefficient	$S_s < 0.05$	$0.05 \leqslant S_s < 0.3$	$0.3 < S_s \leqslant 0.5$	$0.5 < S_s \leqslant 0.7$	$0.7 < S_s \leqslant 1$	$S_s > 1.0$
Sensitivity degree	None	Weak	Moderately weak	Moderately strong	Strong	Extremely strong

Table 3 Evaluation criteria of stress sensitivity by permeability damage rate method

Permeability damage rate/%	$D_k \leqslant 5$	$5 < D_k \leqslant 30$	$30 < D_k \leqslant 50$	$50 < D_k \leqslant 70$	$70 < D_k \leqslant 90$	$D_k > 90$
Sensitivity degree	None	Weak	Moderately weak	Moderately strong	Strong	Extremely strong

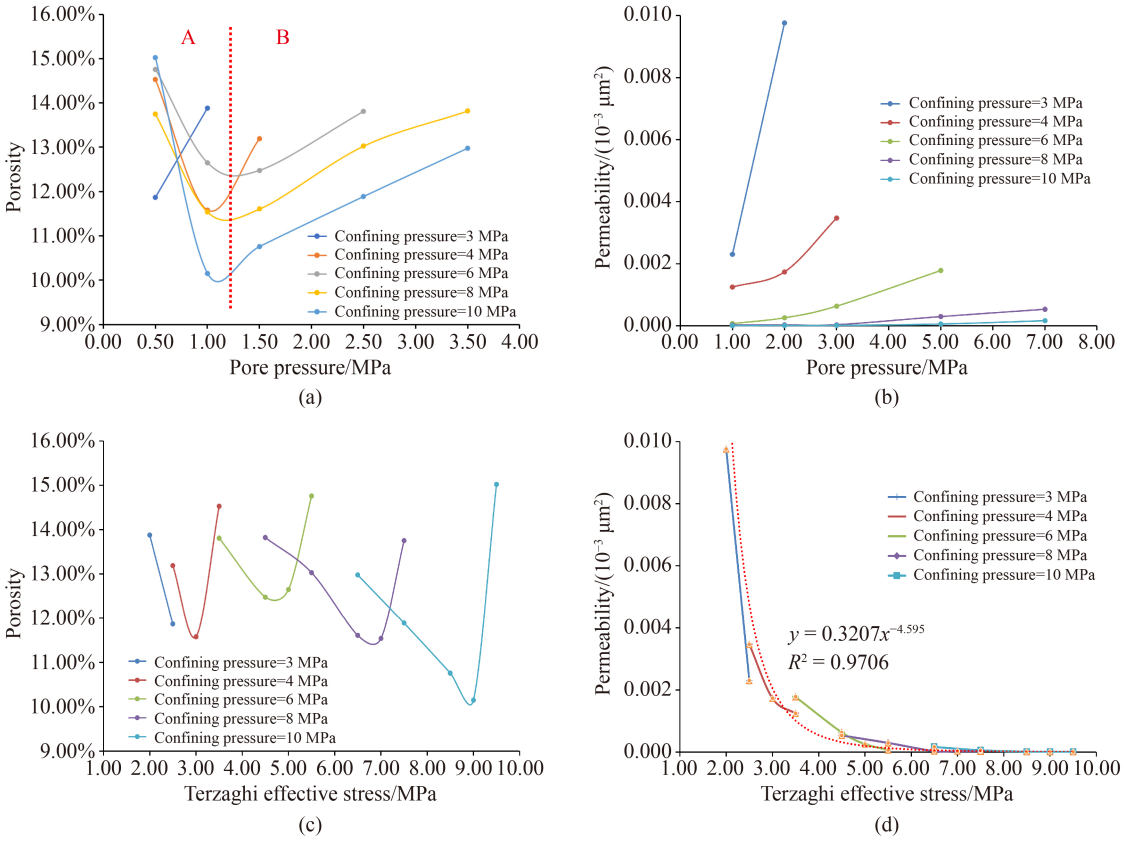

Fig. 4 Experimental results. (a) Relationship between porosity and pore pressure; (b) relationship between permeability and pore pressure; (c) relationship between porosity and Terzaghi effective stress; (d) relationship between permeability and Terzaghi effective stress.

confining pressure. When confining pressure exceeds 6 MPa, the permeability variation is minimal regardless of pore pressure change, which is consistent with previous studies (Zhang et al., 2019a). Figures 4(c) and 4(d) show the comparison between the variation patterns of porosity and permeability, respectively, with increasing effective stress and it can be seen that the stress sensitivity of both porosity and permeability is obvious, and that the Terzaghi effective stress gradually descends with pore pressure ascending at a constant confining pressure. Therefore, the variation patterns of porosity with increasing Terzaghi effective stress are similar to those with decreasing pore pressure (Fig. 4(c)). As shown in Fig. 4(d), the permeability of coal shows a negative exponential decrease with the increase of effective stress, which is a behavior similar to the one concluded by other studies (McKee et al., 1988; Zhang et al., 2017a, 2019a), and is caused due to the significant nonlinear compression of the pore-fracture space. When Terzaghi effective stress exceeds 6 MPa, gas seepage paths are almost completely closed and there is no more obvious change in permeability.

3.2 The porosity sensitivity of coal permeability under different stresses

Both the porosity and permeability of coal are determined by the distribution characteristics of pore-fracture space. Previous work found that the porosity and permeability correlation coefficients of porous media were equal to 3 or a multiple of 3 (Cui and Bustin, 2005; Wang et al., 2013; Shi et al., 2014). The porosity sensitivity coefficient of permeability (C_{PPS}) α_H was calculated using Eq. (3), and the results are marked in Fig. 5.

From the calculation results shown in Fig. 5, it is noticeable that α_H, which reflects the correlation between porosity and coal permeability under different stresses, is a variable with a certain variation trend instead of a

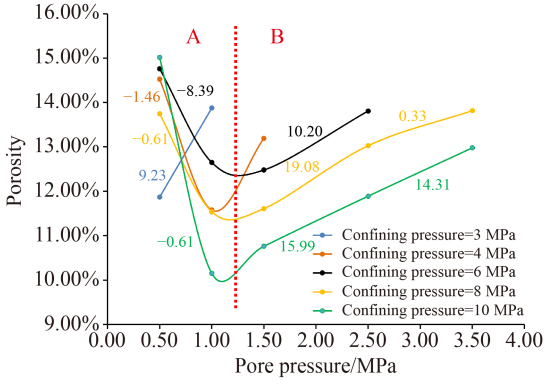

Fig. 5 Porosity sensitivity coefficient of coal permeability.

constant value. We believe that the difference between our results and previous studies can be explained by two factors: the non-homogeneity of coal and the complex distribution of pore-fractures in coal. At the stage of low pore pressure (0–1 MPa), all the α_H values are negative except those at the confining pressure of 3 MPa, indicating that the porosity and permeability of coal were negatively and exponentially correlated with each other. Such a correlation began to turn positive when the pore pressure increased from 1 to 1.5 MPa, while α_H became a high positive value when it kept going up, indicating that the correlation between the porosity and permeability of coal had turned highly positive and exponential.

According to Section 3.1, permeability decreases negatively and exponentially with increasing effective stress, while, in this section, α_H, which is used to characterize the P_{PS} of coal, also varies exponentially rather than linearly, because porosity characterizes the percentage of the total volume occupied by all pore volumes, while permeability characterizes the capability of allowing fluid to pass through and relates only to those seepage pore-fractures. The non-homogeneous compression of a pore-fracture system varies with the change of effective stress, which leads to the irregular change of porosity in stage A. With the increase of pore pressure, the pores without fluid are continuously compressed, while those with fluid make the main contribution to porosity, and the pressure exerted by coal reaches a relative equilibrium with the internal pressure. At this time, there is an obvious positive correlation between porosity and permeability, which is shown by an orderly increase in porosity at stage B.

3.3 Changes in stress sensitivity of coal permeability at different stages

Previously, the stress sensitivity of coal was estimated quantitatively based on M_{PDR} and M_{CSS}, and was classified into six categories, as shown in Tables 2 and 3 (Somerton et al., 1975; Jones and Owens, 1980; Durucan and Edwards, 1986; McKee et al., 1988; Xiao et al., 2016). In CBM production, the effective stress in the coal reservoir changes all along with the fluid discharge, and the stress sensitivity is a continuously changing variable rather than a constant value. Therefore, it is necessary to analyze the variation of stress sensitivity in different stages. Two widely applied methods were used to quantitatively evaluate the stress sensitivity characteristics at different stages of the CBM production.

3.3.1 Permeability damage rate method

Based on D_K calculated using Eq. (5) and M_{PDR}, previous researchers proposed α_k, which refers to the permeability damage rate coefficient (C_{PDR}), to evaluate the stress sensitivity, as shown in Eq. (6) (Meng et al., 2015; Zhang et al., 2019b):

$$\alpha_k = -\frac{\partial k}{k_0 \partial p}, \tag{6}$$

where ∂k is the variation of permeability, 10^{-3} μm^2; ∂p is the variation of effective stress, MPa.

In Fig. 6, the R_{PD} of coal increases significantly with effective stress. The analysis based on Table 3 showed that there was only one value of R_{PD} ranging between 60% and 70% with the effective stress at 2.5 MPa and the confining pressure at 4 MPa, representing moderately strong stress sensitivity, and the rest of the values were greater than 70%, representing strong stress sensitivity. Moreover, the R_{PD} remained greater than 90% with the effective stress higher than 4 MPa, representing extremely strong stress sensitivity.

The change value of permeability damage rate decreases with the increasing confining pressure, which reflects the change of stress sensitivity. To accurately characterize the change in stress sensitivity, the C_{PDR} (α_k) was calculated by Eq. (6) and is shown in Fig. 7. The C_{PDR} of coal dropped dramatically when the effective stress was less than 5–6 MPa, but its descending trend tended to level off and was finally stable around 0.15 when the effective stress was higher than 6 MPa. Most of the seepage space in coal was compressed and closed at this moment.

3.3.2 Stress sensitivity coefficient method

The stress sensitivity coefficient (C_{SS}) of coal was calculated based on Eq. (1) (Fig. 8). According to Table 2, the C_{SS} of all samples is greater than 1, representing extremely strong stress sensitivity. The deviation between the result herein and the conclusion obtained in Section 3.3.1 occurred mainly because the evaluation methods used for them each were different. Nevertheless, there is no doubt that both evaluation methods have proved that the samples have strong stress sensitivity.

As shown in Fig. 8, the C_{SS} exhibits a decreasing trend

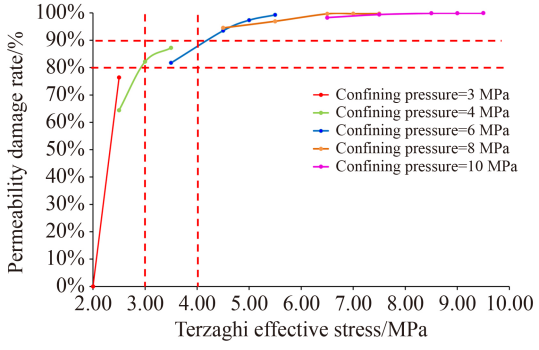

Fig. 6 Relationship between permeability damage rate (R_{PD}) and effective stress.

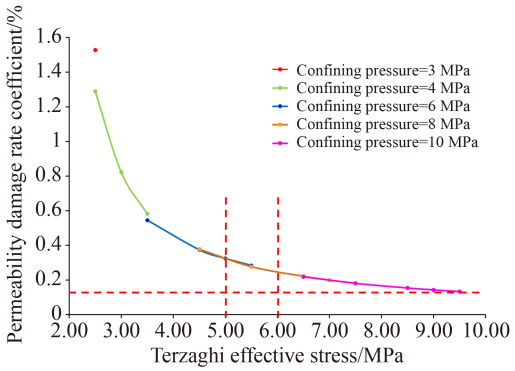

Fig. 7 Relationship between C_{PDR} and effective stress.

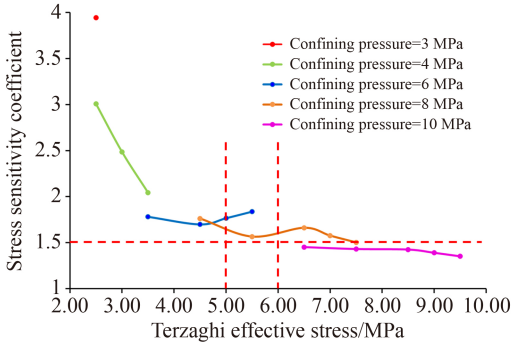

Fig. 8 Relationship between C_{SS} and effective stress.

as the confining pressure increases. The analysis of the C_{SS} change under different confining pressures revealed that C_{SS} only decayed substantially when confining pressure was 3 and 4 MPa, while it started to fluctuate with a minor total reduction in the end when confining pressure became higher. The influence of effective stress on permeability is dominated by seepage paths closed at high effective stress. Most of the pore-fracture space that contributes to the seepage capacity was closed when confining pressure was above 6 MPa and the "fluctuation trend" that occurred afterward was mainly caused by the opening or closing of secondary micro-fractures, which hardly affected the overall trend though. The same conclusion was obtained by previous studies (Meng and Li, 2013; Zhang et al., 2019b).

3.4 Engineering recommendations for CBM production based on stress sensitivity variation

In the production of CBM, the complex transport of gas-water two-phase flow determines the difficulty of the project (Sun et al., 2018). Extensive studies have been conducted by previous researchers to classify the different stages of gas-water two-phase flow (Liu et al., 2015; Clarkson and Qanbari, 2016; Hou et al., 2016). Numerous studies have proved that in CBM production, single-phase water flow transforms into gas-water two-phase flow when the bottom-hole pressure is lower than the critical desorption pressure. The size and expansion rate of the formation pressure drop funnel will affect the production capacity of CBM wells through the stress sensitivity (Xu et al., 2017; Sun et al., 2017). Therefore, the reasonable balance of gas-water two-phase flow changes becomes a critical issue affecting the production of CBM wells.

Section 3.3 discussed the variation of C_{SS} in CBM production rather than using C_{SS} as a value to evaluate the reservoir quantitatively. Since stress sensitivity constantly changes at different stages of CBM well drainage, which undoubtedly increases the difficulty in adjusting the drainage scheme in engineering practice, a detailed analysis is needed for different extraction processes.

The effective stress in a coal reservoir varies all through the process of dewatering and depressurization of CBM wells. When the effective stress goes up due to the discharge of reservoir fluid, the permeability will change drastically, and the stress sensitivity will be the highest. Thus, it is necessary to drain fluid from a reservoir slowly, stably, and continuously to avoid the blockage of seepage paths.

When CH_4 starts desorption with the reservoir pressure approaching the critical desorption pressure, the reservoir is saturated with less water and more gas. The reduction rate of C_{SS} tends to level off gradually, but permeability is still highly impacted by C_{SS}. Hence, the gas-water dynamic equilibrium formed in the previous stage must be maintained to avoid blockage by gas or water.

With the continuous desorption of CH_4, the coal matrix shrinks significantly, and permeability increases. Besides, the water saturation approaches the minimum value, and the pore pressure is almost entirely provided by CH_4. Meanwhile, C_{SS} also goes down toward the minimum value and then gradually becomes stable. Finally, the CBM well production begins to increase and will enter the period of stable gas production.

In conclusion, it is necessary to establish a dynamic equilibrium of fluid pressure inside a reservoir by adjusting the drainage volume and extraction rate to ensure smooth extraction from a CBM well with complex stress change, which will minimize the influence of stress sensitivity on permeability.

4 Conclusions

To comprehensively analyze the coupling effect of the pore system and permeability with stress controlled during the production of a CBM well, porosity and permeability experiments under different confining and pore pressures were set up by simulating the production state of a CBM well. The conclusions are as follows.

1) At an equal pore pressure, porosity decreases as confining pressure increases, and shows a first ascending and then descending trend when pore pressure increases at a constant confining pressure. Besides, the porosity at the final stage is always lower than that at the initial stage

because part of the pore-fracture space has been irreversibly closed.

2) In all tests with different confining pressures, permeability increased with pore pressure and its increment showed a negative correlation with confining pressure. Besides, the coal permeability decreased negatively and exponentially with effective stress increasing until it approached a minimum value and then hardly changed when effective stress was greater than 6 MPa, mainly because effective seepage paths of CH_4 were reduced due to the compression of pore-fracture space.

3) The correlation between permeability and porosity is stage-specific. With pore pressure increasing, the value of C_{PPS} changed from negative to positive and went through three stages: the negative exponential relationship stage, the adjustment stage, and the positive exponential relationship stage.

4) The dynamic change of stress sensitivity during CBM well drainage was evaluated by two methods and it was proved that the reduction rate of C_{SS} gradually went down when effective stress increased, which provides technical support for the CBM development.

Acknowledgments This research was funded by the National Natural Science Foundation of China (Grant No. 41872170), the National Major Special Project of Science and Technology of China (No. 2016ZX05044), and the Fundamental Research Funds for the Central Universities (No. 2020CXNL11).

References

Ai T, Wu S, Zhang R, Gao M, Zhou J, Xie J, Ren L, Zhang Z (2021). Changes in the structure and mechanical properties of a typical coal induced by water immersion. Int J Rock Mech Min Sci, 138: 104597

Aziz N, Ren T, Nemcik J, Zhang L (2013). Permeability and volumetric changes in coal under different test environment. Acta Geodyn Geomater, 10: 163–171

Chen S, Liu P, Tang D, Tao S, Zhang T (2021a). Identification of thin-layer coal texture using geophysical logging data: investigation by Wavelet Transform and Linear Discrimination Analysis. Int J Coal Geol, 239: 103727

Chen S, Tang D, Tao S, Liu P, Mathews J P (2021b). Implications of the in situ stress distribution for coalbed methane zonation and hydraulic fracturing in multiple seams, western Guizhou, China. J Petrol Sci Eng, 204: 108755

Chen S, Tao S, Tian W, Tang D, Zhang B, Liu P (2021c). Hydrogeological control on the accumulation and production of coalbed methane in the Anze Block, southern Qinshui Basin, China. J Petrol Sci Eng, 198: 108138

Chen Y, Liu D, Yao Y, Cai Y, Chen L (2015). Dynamic permeability change during coalbed methane production and its controlling factors. J Nat Gas Sci Eng, 25: 335–346

Chen Z, Liu J, Pan Z, Connell L D, Elsworth D (2012). Influence of the effective stress coefficient and sorption-induced strain on the evolution of coal permeability: model development and analysis. Int J Greenh Gas Control, 8: 101–110

Chen Z, Pan Z, Liu J, Connell L D, Elsworth D (2011). Effect of the effective stress coefficient and sorption-induced strain on the evolution of coal permeability: experimental observations. Int J Greenh Gas Control, 5(5): 1284–1293

Clarkson C R, Qanbari F (2016). A semi-analytical method for forecasting wells completed in low permeability, undersaturated CBM reservoirs. J Nat Gas Sci Eng, 30: 19–27

Cui X, Bustin R M (2005). Volumetric strain associated with methane desorption and its impact on coalbed gas production from deep coal seams. AAPG Bull, 89(9): 1181–1202

Durucan S, Edwards J S (1986). The effects of stress and fracturing on permeability of coal. Min Sci Technol, 3(3): 205–216

Geng Y, Tang D, Xu H, Tao S, Tang S, Ma L, Zhu X (2017). Experimental study on permeability stress sensitivity of reconstituted granular coal with different lithotypes. Fuel, 202: 12–22

Gu F, Chalaturnyk R (2010). Permeability and porosity models considering anisotropy and discontinuity of coalbeds and application in coupled simulation. J Petrol Sci Eng, 74(3–4): 113–131

Guo P, Cheng Y, Jin K, Li W, Tu Q, Liu H (2014). Impact of effective stress and matrix deformation on the coal fracture permeability. Transp Porous Media, 103(1): 99–115

Guo X, Zou G, Wang Y, Wang Y, Gao T (2017). Investigation of the temperature effect on rock permeability sensitivity. J Petrol Sci Eng, 156: 616–622

Han J, Wu C, Jiang X, Fang X, Zhang S (2022). Investigation on effective stress coefficients and stress sensitivity of different water-saturated coals using the response surface method. Fuel, 316: 123238

Hou P, Gao F, Ju Y, Cheng H, Gao Y, Xue Y, Yang Y (2016). Changes in pore structure and permeability of low permeability coal under pulse gas fracturing. J Nat Gas Sci Eng, 34: 1017–1026

Jasinge D, Ranjith P G, Choi S K (2011). Effects of effective stress changes on permeability of latrobe valley brown coal. Fuel, 90(3): 1292–1300

Jones F O, Owens W W (1980). A laboratory study of low-permeability gas sands. J Pet Technol, 32(9): 1631–1640

Ju Y, Zhang Q, Zheng J, Wang J, Chang C, Gao F (2017). Experimental study on CH_4 permeability and its dependence on interior fracture networks of fractured coal under different excavation stress paths. Fuel, 202: 483–493

Li Y, Tang D, Xu H, Meng Y, Li J (2014). Experimental research on coal permeability: the roles of effective stress and gas slippage. J Nat Gas Sci Eng, 21: 481–488

Liu H, Rutqvist J (2010). A new coal-permeability model: internal swelling stress and fracture–matrix interaction. Transp Porous Media, 82(1): 157–171

Liu J, Chen Z, Elsworth D, Miao X, Mao X (2011a). Evolution of coal permeability from stress-controlled to displacement-controlled swelling conditions. Fuel, 90(10): 2987–2997

Liu J, Wang J, Chen Z, Wang S, Elsworth D, Jiang Y (2011b). Impact of transition from local swelling to macro swelling on the evolution of coal permeability. Int J Coal Geol, 88(1): 31–40

Liu T, Lin B, Yang W (2017). Impact of matrix–fracture interactions on coal permeability: model development and analysis. Fuel, 207: 522–532

Liu W, Liu Y, Niu C, Han G, Wan Y (2015). A model of unsteady seepage flow in low-permeable coalbed with moving boundary in consideration of wellbore storage and skin effect. Procedia Eng, 126: 517–521

McKee C R, Bumb A C, Koenig R A (1988). Stress-dependent permeability and porosity of coal and other geologic formations. SPE Form Eval, 3(1): 81–91

Meng Y, Li Z, Lai F (2015). Experimental study on porosity and permeability of anthracite coal under different stresses. J Petrol Sci Eng, 133: 810–817

Meng Y, Liu S, Li Z (2018). Experimental study on sorption induced strain and permeability evolutions and their implications in the anthracite coalbed methane production. J Petrol Sci Eng, 164: 515–522

Meng Z, Li G (2013). Experimental research on the permeability of high-rank coal under a varying stress and its influencing factors. Eng Geol, 162: 108–117

Mitra A, Harpalani S, Liu S (2012). Laboratory measurement and modeling of coal permeability with continued methane production: part I – laboratory results. Fuel, 94: 110–116

Niu Y, Mostaghimi P, Shikhov I, Chen Z, Armstrong R T (2018). Coal permeability: gas slippage linked to permeability rebound. Fuel, 215: 844–852

Özgül N M, Savaşçın M, Özkan İ (2017). Recycling of coal ash in production of low density masonry unit. Acta Phys Pol A, 132(3): 430–432

Pan Z, Connell D, Camilleri M (2010). Laboratory characterisation of coal reservoir permeability for primary and enhanced coalbed methane recovery. Int J Coal Geol, 82(3–4): 252–261

Shao J, You L, Kang Y, Gao X, Chen M, Meng S, Zhang N (2020). Experimental study on stress sensitivity of underground gas storage. J Petrol Sci Eng, 195: 107577

Shaw D, Mostaghimi P, Armstrong R T (2019). The dynamic behaviour of coal relative permeability curves. Fuel, 253: 293–304

Shi J, Durucan S, Shimada S (2014). How gas adsorption and swelling affects permeability of coal: a new modelling approach for analysing laboratory test data. Int J Coal Geol, 128–129: 134–142

Somerton W H, Söylemezoğlu I M, Dudley R C (1975). Effect of stress on permeability of coal. Intern J Rock Mechanics Mining Sci Geomechanics. Elsevier: 129–145

Sun Z, Li X, Shi J, Yu P, Huang L, Xia J, Sun F, Zhang T, Feng D (2017). A semi-analytical model for drainage and desorption area expansion during coal-bed methane production. Fuel, 204: 214–226

Sun Z, Shi J, Wang K, Miao Y, Zhang T, Feng D, Sun F, Wang S, Han S, Li X (2018). The gas-water two phase flow behavior in low-permeability CBM reservoirs with multiple mechanisms coupling. J Nat Gas Sci Eng, 52: 82–93

Tao S, Chen S, Pan Z (2019a). Current status, challenges, and policy suggestions for coalbed methane industry development in China: a review. Energy Sci Eng, 7(4): 1059–1074

Tao S, Chen S, Tang D, Zhao X, Xu H, Li S (2018). Material composition, pore structure and adsorption capacity of low-rank coals around the first coalification jump: a case of eastern Junggar Basin, China. Fuel, 211: 804–815

Tao S, Pan Z, Tang S, Chen S (2019b). Current status and geological conditions for the applicability of CBM drilling technologies in China: a review. Int J Coal Geol, 202: 95–108

Wang G, Ren T, Wang K, Zhou A (2014a). Improved apparent permeability models of gas flow in coal with Klinkenberg effect. Fuel, 128: 53–61

Wang J, Tang D, Xu H, Yi J, Yi Y (2013). Stress sensitivity of coal samples in terms of anisotropy. J Coal Sci Eng China, 19(2): 203–209

Wang K, Zang J, Wang G, Zhou A (2014b). Anisotropic permeability evolution of coal with effective stress variation and gas sorption: model development and analysis. Int J Coal Geol, 130: 53–65

Wang S, Elsworth D, Liu J (2011). Permeability evolution in fractured coal: The roles of fracture geometry and water-content. Int J Coal Geol, 87(1): 13–25

Wang S, Li H, Wang W, Li D (2018a). Experimental study on mechanical behavior and energy dissipation of anthracite coal in natural and forced water-saturation states under triaxial loading. Arab J Geosci, 11(21): 668

Wang W, Li H, Liu Y, Liu M, Wang H, Li W (2020). Addressing the gas emission problem of the world's largest coal producer and consumer: lessons from the Sihe Coalfield, China. Energy Rep, 6: 3264–3277

Wang W, Wang H, Li D, Li H, Liu Z (2018b). Strength and failure characteristics of natural and water-saturated coal specimens under static and dynamic loads. Shock Vib, 2018: 1–15

Xiao K, Zhang Z, Zhang R, Gao M, Xie J, Zhang A, Liu Y (2021). Anisotropy of the effective porosity and stress sensitivity of coal permeability considering natural fractures. Energy Rep, 7: 3898–3910

Xiao W, Li T, Li M, Zhao J, Zheng L, Li L (2016). Evaluation of the stress sensitivity in tight reservoirs. Pet Explor Dev, 43(1): 115–123

Xie H, Ju Y, Gao F, Gao M, Zhang R (2017). Groundbreaking theoretical and technical conceptualization of fluidized mining of deep underground solid mineral resources. Tunn Undergr Space Technol, 67: 68–70

Xu B, Li X, Ren W, Chen D, Chen L, Bai Y (2017). Dewatering rate optimization for coal-bed methane well based on the characteristics of pressure propagation. Fuel, 188: 11–18

Yao Y, Liu D, Xie S (2014). Quantitative characterization of methane adsorption on coal using a low-field NMR relaxation method. Int J Coal Geol, 131: 32–40

Ye J, Tao S, Zhao S, Li S, Chen S, Cui Y (2022). Characteristics of methane adsorption/desorption heat and energy with respect to coal rank. J Nat Gas Sci Eng, 99: 104445

Zhang X, Wu C, Liu S (2017a). Characteristic analysis and fractal model of the gas-water relative permeability of coal under different confining pressures. J Petrol Sci Eng, 159: 488–496

Zhang X, Wu C, Wang Z (2019a). Experimental study of the effective stress coefficient for coal permeability with different water saturations. J Petrol Sci Eng, 182: 106282

Zhang Y, Xu X, Lebedev M, Sarmadivaleh M, Barifcani A, Iglauer S (2016a). Multi-scale x-ray computed tomography analysis of coal

microstructure and permeability changes as a function of effective stress. Int J Coal Geol, 165: 149–156

Zhang Z, Zhang R, Wu S, Deng J, Zhang Z, Xie J (2019b). The stress sensitivity and porosity sensitivity of coal permeability at different depths: a case study in the Pingdingshan mining area. Rock Mech Rock Eng, 52(5): 1539–1563

Zhang Z, Zhang R, Xie H, Gao M, Xie J (2016b). Mining-induced coal permeability change under different mining layouts. Rock Mech Rock Eng, 49(9): 3753–3768

Zhang Z, Zhang R, Xie H, Gao M, Zha E, Jia Z (2017b). An anisotropic coal permeability model that considers mining-induced stress evolution, microfracture propagation and gas sorption-desorption effects. J Nat Gas Sci Eng, 46: 664–679

Zhang Z, Zhang R, Xie H, Gao M (2015). The relationships among stress, effective porosity and permeability of coal considering the distribution of natural fractures: theoretical and experimental analyses. Environ Earth Sci, 73(10): 5997–6007

Zhao Y, Liu S, Jiang Y, Wang K, Huang Y (2016). Dynamic tensile strength of coal under dry and saturated conditions. Rock Mech Rock Eng, 49(5): 1709–1720